PHYSICAL REVIEW B **79**, 161406(R) (2009)

Resonantly suppressed transmission and anomalously enhanced light absorption in periodically modulated ultrathin metal films

I. S. Spevak,[1] A. Yu. Nikitin,[1,2] E. V. Bezuglyi,[3] Alex Levchenko,[4] and A. V. Kats[1,*]

[1]*A. Ya. Usikov Institute for Radiophysics and Electronics NASU, 61085 Kharkov, Ukraine*

[2]*Departamento de Física de la Materia Condensada and Instituto de Ciencia de Materiales de Aragón, CSIC-Universidad de Zaragoza, E-50009 Zaragoza, Spain*

[3]*B. I. Verkin Institute for Low Temperature Physics NASU, 61103 Kharkov, Ukraine*

[4]*Department of Physics, University of Minnesota, Minneapolis, Minnesota 55455, USA*

(Received 19 November 2008; published 27 April 2009)

We study light diffraction in the periodically modulated ultrathin metal films both analytically and numerically. Without modulation, these films are almost transparent. The periodicity results in the anomalous effects, such as *suppression of the transmittance* accompanied by a strong enhancement of the absorptivity and specular reflectivity, due to the excitation of the surface-plasmon polaritons. These phenomena are opposite to the widely known *enhanced transparency* of periodically modulated optically thick metal films. Our theoretical analysis can be a starting point for the experimental investigation of these intriguing phenomena.

DOI: 10.1103/PhysRevB.79.161406 PACS number(s): 42.25.−p, 73.20.Mf, 78.20.Bh, 78.20.Ci

Ten years ago Ebbesen *et al.*[1] reported on a pioneering observation of the *enhanced light transmission* through subwavelength hole arrays. Now being classical, this experiment stimulated a large number of investigations focused on the diffraction by the optically thick metal films which were periodically modulated by holes, slits, surface corrugations, etc. The physical origin of the enhanced light transmission is the interaction between the eigenmodes of an opaque metal film and the incoming and outgoing waves.[2] More specifically, periodic modulation leads to the transformation of incoming photons into surface-plasmon polaritons (SPPs) localized at the film interfaces. The subsequent back transformation of the excited SPPs into outgoing photons[3–5] gives rise to the observed anomalous effects in the light reflection and transmission.

In this Rapid Communication, we predict an opposite unexpected effect: highly transparent ultrathin films with the thickness ℓ smaller or comparable to the skin depth δ, being periodically modulated, become nearly *opaque and high reflective* within a certain frequency region which is blue shifted with respect to the local transmittance maximum. Another amazing feature of the predicted phenomenon is an extraordinary enhanced absorptivity (up to 50%) in a narrow vicinity of the maximum of the amplitude of the resonantly excited SPP wave. This *resonance point* is located between the transmittance maximum and minimum (Fano profile).

To clarify the most essential physics of the effect, we examine the simplest case of one-dimensional modulation with symmetric dielectric surrounding. In our analytical approach, we develop a resonance perturbation theory based on the small parameter $\ell/\delta \ll 1$. An analogous approach (with periodic modulation supposed to be a small parameter) has been successfully used in studies of the resonant diffraction in periodically modulated metal half spaces and thick films.[6–9] Additional simplifications are provided by large negative values of the real part of the complex dielectric permittivity $\varepsilon=\varepsilon'+i\varepsilon''$, $|\varepsilon'| \gg 1$, along with smallness of the absorption, $\varepsilon'' \ll |\varepsilon'|$. These conditions are typical for noble and some other metals in visible and near-infrared spectral regions. Our analytical results are supported by the numerical analysis.

Consider a plane monochromatic TM-polarized wave, with magnetic field $\mathbf{H}^i(x,z)=\hat{\mathbf{y}}\exp(i\mathbf{k}^i\mathbf{r})$, incident onto the periodically modulated metal film with the grating period d, as shown in Fig. 1. The wave vector of the incident wave $\mathbf{k}^i=k\sqrt{\varepsilon_d}(\sin\theta, 0, \cos\theta)$, where $k=\omega/c$, ε_d is the dielectric permittivity of the surrounding medium, and θ denotes the angle of incidence. We represent the diffracted magnetic field in the half spaces $z\leq 0$, $z\geq \ell$ in the form of the Fourier-Floquet expansion,

$$H(x,z)=\sum_n \exp(iq_n x)\begin{cases} R_n e^{if(q_n)z}, & z\leq 0 \\ T_n e^{-if(q_n)(z-\ell)}, & z\geq \ell, \end{cases} \tag{1}$$

where $f(q)\equiv\sqrt{\varepsilon_d k^2-q^2}$ with $\mathrm{Re},\mathrm{Im}\, f(q)\geq 0$, $q_n=k\sqrt{\varepsilon_d}\sin\theta+ng$, $n=0,\pm 1,\ldots$, $g=2\pi/d$ is the period of the reciprocal lattice, and the time dependence $\exp(-i\omega t)$ is omitted. R_n and T_n are the reflection and transmission transformation coefficients (TCs), respectively. Inside the film, $0\leq z\leq \ell$, the fields are

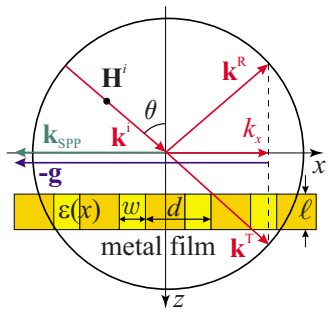

FIG. 1. (Color online) Geometry of the resonant diffraction problem. $\mathbf{k}^i$, $\mathbf{k}^R$, and $\mathbf{k}^T$ are the wave vectors of the incident, specularly reflected, and zero-order transmitted waves, respectively; $\mathbf{k}_{\mathrm{SPP}}$ is the wave vector of the excited SPP, $\mathbf{g}$ is the reciprocal grating vector, d is the grating period, and w is the slit width.

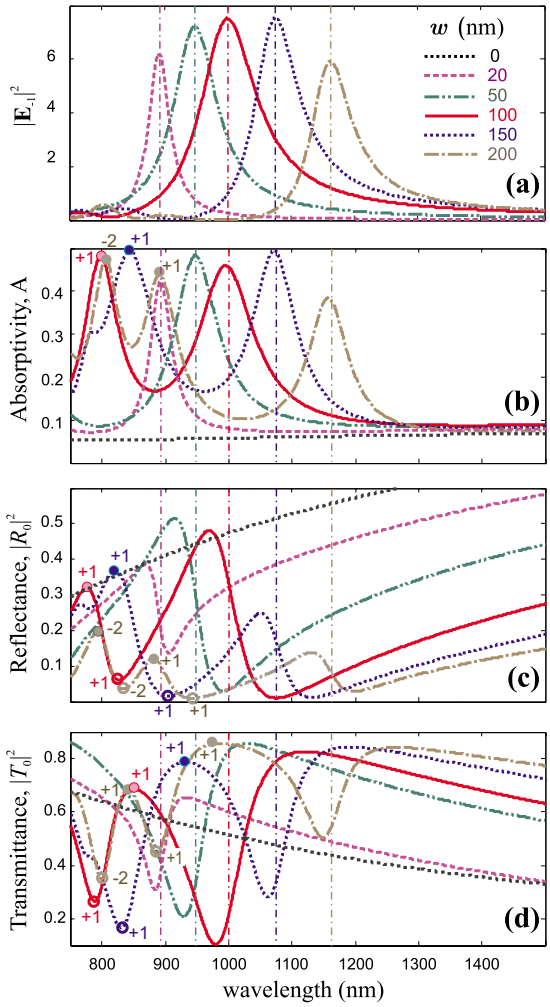

FIG. 2. (Color online) Wavelength dependence (a) of the intensity of the −1st-order diffracted wave at the film boundary, (b) total absorptivity, (c) zero diffraction order reflectance, and (d) transmittance (numerical calculation). The parameters are $\varepsilon_d=1$, $\varepsilon_{\text{lamel}}=\varepsilon_{\text{gold}}$, $\varepsilon_{\text{slit}}=0.2\varepsilon_{\text{gold}}$, the incident angle $\theta=45°$, the grating period $d=400$ nm, the film thickness $\ell=10$ nm, and the slit width w is shown in the legend in (a). Vertical dash-dotted lines indicate the position of the SR resonance in $r=-1$ diffraction order; open (filled) circles indicate minima (maxima) of $|R_0|$ and $|T_0|$ for the $r=1$ and $r=-2$ resonances. The longest-wavelength extremes (not marked) correspond to the $r=-1$ resonance.

$$\{H(x,z),\mathbf{E}(x,z)\}=\sum_n \{H_n(z),\mathbf{E}_n(z)\}\exp(iq_n x). \tag{2}$$

Excluding the normal component of the electric field by means of the Maxwell equations, we obtain a set of the first-order linear ordinary differential equations for the functions $H_n(z)$ and $E_{xn}(z)$. The solution of this set couples the values of the internal fields on the interfaces. By matching the fields at the interfaces, we obtain an infinite set of linear algebraic equations for R_n and T_n.

Before proceeding with the analytical treatment, we present an example of numerical calculations of the resonant spectral properties of a periodically modulated ultrathin film (Fig. 2). The calculations have been performed by the rigorous coupled wave analysis (RCWA) (cf. Refs. 10 and 11) We assume an opaque filling of the slits which restricts the resonances to the SPP modes only and prevents other resonances (e.g., slit modes). Note that the opaque material of the filling does not qualitatively influence the results. Therefore, it is sufficient to chose a high contrast but opaque filling resulting in strong resonances even for small slit widths. The gold permittivity is taken in the form of the Drude-Lorentz model according to Ref. 12. This model has shown to have a reasonable agreement with the experiments not only for thick metal films but also for very thin films (down to 8 nm) (see, e.g., Ref. 3).

Figure 2 shows that the transmittance $|T_0|^2$, absorptivity A, and reflectance $|R_0|^2$ possess strong resonant behavior for various slit widths w in the spectral region typical for the experiments. Depending on the slit width, the transmittance in the resonance region is suppressed up to 10% for $\ell=10$ nm, whereas it is on the order of 85% away from the resonance. In contrast, the reflectance and absorption are greatly enhanced up to 50%. It turns out that all shown peculiarities are related to the resonant excitation of the short-range (SR) SPP (Refs. 3–5) in a certain diffraction order. Namely, the longest-wavelength extremes of $|R_0|^2$, $|T_0|^2$, and A correspond to the −1st SR SPP resonance shown in Fig. 2(a), while the short-wavelength extremes are due to the +1st and −2nd resonances. We stress that due to the oblique incidence, the excited resonances are far away from the band gaps, i.e., we are dealing with "single" resonances.

In order to explain quantitatively the resonant peculiarities of the spectra, we consider analytically the solution in the vicinity of a single SR resonance. To this end, we solve the set of equations for the field amplitudes in the resonant approximation[6–9] using the small parameter $\ell/\delta=k\ell\sqrt{|\varepsilon|}\ll 1$. The resonances correspond to the excitation of both SR and long-range (LR) SPP modes. However, as it follows from the analytical considerations and is confirmed by the computations, just the excitation of SR SPP strongly affects energy fluxes of the outgoing waves. Within the second order in $k\ell$, we obtain the resonant TC in the vicinity of a single SR resonance in rth diffraction order,

$$R_r=-\frac{u_0}{u_0+2i}\frac{\mathbb{E}_{r0}}{\mathbb{E}_{00}}\frac{1}{F_r/F_{\text{SR}}-1},\quad T_r\simeq -R_r, \tag{3}$$

where

$$F_m=f(q_m)/(k\sqrt{\varepsilon_d}),\quad u_m=k\ell\mathbb{E}_{mm}F_m,\quad F_{\text{SR}}=2/ik\ell Z_r, \tag{4}$$

$$Z_r=\mathbb{E}_{rr}+ik\ell X_r,\quad X_r=\sum_{N\neq r}\frac{F_N\mathbb{E}_{rN}\mathbb{E}_{Nr}}{2-iu_N}. \tag{5}$$

Here $\hat{\mathbb{E}}=\hat{\zeta}^{-1}$, where the elements of the Töplitz matrix $\hat{\zeta}$ are formed by the Fourier coefficients of $1/\varepsilon(x)$ expansion, $\zeta_{mn}=(1/\varepsilon)_{m-n}$ (Refs. 10 and 11).

The resonant TC is proportional to the modulation harmonic which couples the incident wave with SPP through a one-step scattering. Other scattering processes contribute to the denominator of R_r. The pole of R_r corresponds to the SR

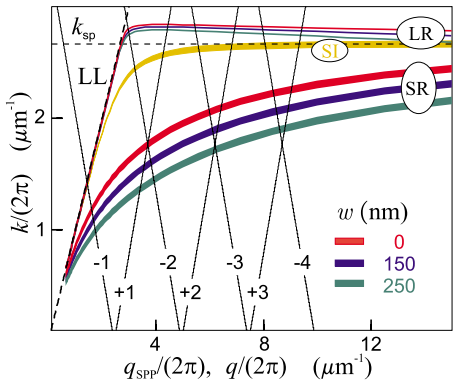

FIG. 3. (Color online) Dispersion curves for SPPs at the air/gold single interface (SI) and for the SR and LR SPPs for a homogeneous film with mean permittivity ε_0 for different slit widths and $\ell=10$ nm. The thickness of these curves reflects the SPP linewidth. The light line (LL) is shown in black dash. The dashed horizontal line indicates the surface-plasmon frequency, $k_{sp}=\omega_{sp}/(2\pi c)$, $\varepsilon'(\omega_{sp})=-1$. Numbered lines are $q=|q_n|=|k\sin\theta+ng|$ with $n=\pm1,\ldots$ for $\theta=45°$. Intersection of the nth line with the dispersion curve corresponds to the resonance excitation of the SPP in nth diffraction order.

SPP dispersion relation $q_{SR}^2\simeq\varepsilon_d k^2[1+4/(k\ell Z_r)^2]$ modified by a periodic modulation. This modification is governed by the real part of Z_r, $Z_r'\simeq\varepsilon_0'-k\ell X_r''$, which is basically determined by the first term. This explains naturally the redshift of the resonant peculiarities with increasing slit width w (see Fig. 2). Indeed, when w increases, $|\varepsilon_0'|$ decreases and forces the redshift of the SPP dispersion relation, as demonstrated in Fig. 3.

The dissipation and SPP linewidth are governed by the imaginary part of Z_r, $Z_r''\simeq\varepsilon_0''+k\ell X_r'$. Here the second term exceeds the first one even for a moderate modulation. We emphasize that the second term is mainly determined by the summation over outgoing waves [in Eq. (5)] responsible for SPP radiative losses (leakage). We show in Fig. 4(a) an example of the resonant field amplitude calculated from Eqs. (3)–(5) for $r=-1$.

Due to the excitation of SR SPP, R_r approaches maximum in the vicinity of the SPP pole at the point $F_r=F_{SR}$ [see Figs. 2(a) and 4(a)]. In view of $\varepsilon''\ll|\varepsilon'|$, the pole is close to the imaginary axis in the complex F_r plane. The condition $\mathrm{Im}[F_r(\lambda,\theta)]=\mathrm{Im}[F_{SR}(\lambda,\theta)]$ yields the local maximum of $|R_r|$ in (λ,θ) plane. Along this *resonance line*, we have

$$|R_r|^2_{\max}\simeq\frac{|u_0|^2}{|u_0|^2+4}\left|\frac{\mathbb{E}_{r0}}{\mathbb{E}_{00}}\right|^2\left(\frac{Z_r'}{Z_r''}\right)^2. \tag{6}$$

To study the far field, the knowledge of the nonresonant-order TCs is necessary. In general, not only the zero order but also other diffracted orders contribute to the far-field energy flux. Within our analytical approach, they are given by

$$R_N=\bar{R}_N+\delta R_N,\quad T_N=\bar{T}_N-\delta R_N,\quad N\neq r, \tag{7}$$

where $\bar{R}_N$, $\bar{T}_N$ are contributions from the nonresonant scattering processes,

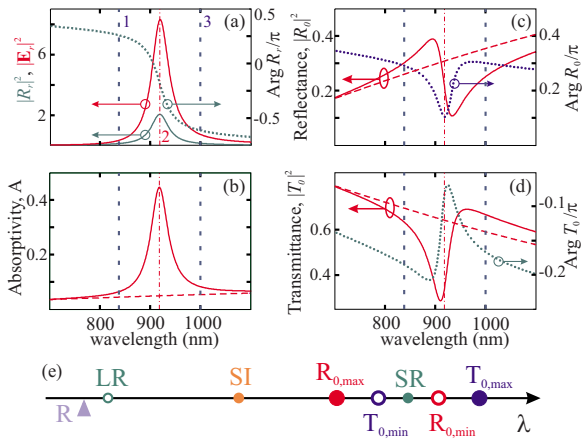

FIG. 4. (Color online) Results of analytical calculations for $r=-1$ resonance: wavelength dependence of the (a) resonant wave magnitude and phase, (b) total absorptivity, (c) zero-order reflectance, (d) and transmittance for the slit width $w=100$ nm; other parameters are the same as in Fig. 2. Vertical lines 1–3 indicate the wavelengths of SR SPP for slitless gold film (1) and the SR SPP resonance for modulated film calculated analytically (2) and numerically (3) (cf. Fig. 2). Dash lines in (b)–(d) show quantities for a homogeneous film with the mean permittivity value. The typical ordering of the Rayleigh point R, the LR, SI, SR SPP resonances, and the extreme points for the zero-order reflectance and transmittance are shown in (e).

$$\bar{R}_N=\frac{k\ell F_0\mathbb{E}_{N0}}{u_N+2i},\quad \bar{T}_N=\delta_{N,0}-\bar{R}_N, \tag{8}$$

and δR_N is the resonant contribution coming from the SR SPP backscattering into the nonresonant diffraction orders,

$$\delta R_N=-k\ell\frac{(F_r-ik\ell/2)\mathbb{E}_{Nr}}{u_N+2i}R_r. \tag{9}$$

For zero-order TCs, T_0 and R_0, the nonresonant terms coincide with corresponding Fresnel coefficients $\bar{T}_0$ and $\bar{R}_0$ for the film with mean value of the dielectric permittivity $\mathbb{E}_{00}\simeq\varepsilon_0$. Spectral dependences of $|\bar{T}_0|^2$ and $|\bar{R}_0|^2$ are shown by dash lines in Figs. 4(c) and 4(d). Thus, T_0 and R_0 result from the interference between the resonant and direct (nonresonant) channels. This interference leads to neighboring minima and maxima in both $|R_0|$ and $|T_0|$ (Fano profile) [see panels (c) and (d) in Figs. 4 and 2]. According to Eqs. (7)–(9), the maximum of $|T_0|^2$ lies to the right from the above-indicated resonant point, whereas the minimum lies to the left. The maximum of $|T_0|^2$ is accompanied by the complementary minimum of $|R_0|^2$ and vice versa. Positions of these complementary extrema are slightly different, as shown in Fig. 4(e). The resonance also results in the absorption maximum (in the close vicinity of $|R_r|^2$ maximum) (cf. Figs. 4 and 2). Noteworthy, even for small active losses, $\varepsilon''\ll|\varepsilon'|$, the absorption, being small for ultrathin unmodulated films, increases substantially (up to 50%) for an appropriate modulation.

Consider now in detail the case of $r=-1$ resonance. It is well separated from other resonances at oblique incidence.

Moreover, only zero-order diffracted waves are outgoing and contribute to the far field. This leads to the reduction in the radiative losses and resonant linewidth as compared with other resonances. One can see from Eq. (6) and Fig. 2(a) that the spectral maximum of the resonance-order intensity depends nonmonotonously on the modulation (e.g., on the slit width). The intensity is maximal at $|\mathbb{E}_{r0}|=\mathcal{E}$, when the dissipation losses are equal to the radiative ones, i.e.,

$$\mathcal{E}^2 = \frac{|u_0|^2+4}{2|u_0|}\mathbb{E}''_{00}|\mathbb{E}_{00}|, \quad r=-1. \tag{10}$$

Substitution of $\mathcal{E}$ into Eq. (6) yields $|R_r|^2_{\max} \to |R_r|^2_{\text{extreme}} \simeq |u_0\mathbb{E}_{00}|/(8\mathbb{E}''_{00}) \gg 1$. For the modulation level given by Eq. (10), we obtain $T_0=R_0=1/2$, and the absorptivity approaches the maximal value 0.5 in the resonance. For slit structure with $\varepsilon_d=1$, $\varepsilon_{\text{lamel}}=\varepsilon_{\text{gold}}$, $\varepsilon_{\text{slit}}=0.2\varepsilon_{\text{gold}}$, and $\theta=45°$, Eq. (10) gives the optimal value $w/d \simeq 1/4$ which well agrees with the numerical simulations (cf. Fig. 2).

The minimum value of the transmittance also depends nonmonotonously on the slit width. This minimum can be very low (specifically, for transparent slits it may fall to few percents). The minimal value of the zero-order transmittance is determined by the sum of the dissipative and radiative losses in nonzero-order diffraction channels. For $r=-1$ resonance, the nonzero-order radiative losses are absent, and the transmittance falls up to $|T_0|_{\min} \propto \varepsilon''_0/|\varepsilon_r| \ll 1$.

The discussed effect of the transmittance suppression is illustrated in Fig. 5. Here we show the instant distribution of the magnetic field $\text{Re}[H(x,z)]$ for two values of the wavelength related to the minimum and maximum of the transmittance [cf. Figs. 2(c) and 2(d)]. The transmittance minimum is accompanied by the reflectance maximum. As a result, the high-contrast interference pattern appears [see Fig. 5(a)]. On the other hand, the transmittance maximum is accompanied by the reflectance minimum resulting in almost complete disappearance of the interference [Fig. 5(b)].

The predicted phenomena hold true for films of other good metals (say, Ag and Cu) and for higher film thicknesses. For gold 20-nm-thick film, they are even more deep and contrast. With the absorption increase the effects become less pronounced, however, they are still well noticed even when the absorption increases two to three times.

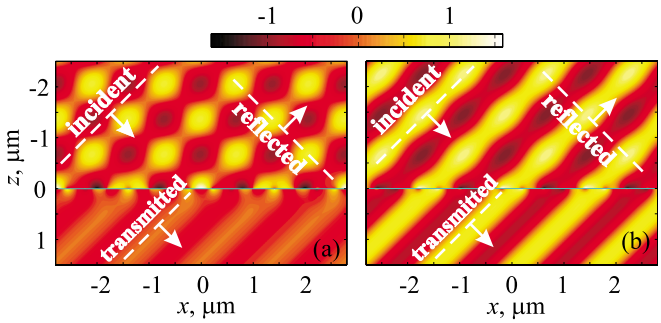

FIG. 5. (Color online) Spatial distribution of the magnetic field $\text{Re}[H(x,z)]$ for $w=100$ nm, $\lambda=980$ nm in (a), and $\lambda=1122$ nm in (b). These wavelengths correspond to the transmittance minimum and maximum, respectively, which are caused by SPP resonance in -1st diffraction order. Other parameters are the same as in Fig. 2.

In conclusion, we have predicted the extraordinary resonant properties of ultrathin periodically modulated metal films. In contrast to the widely discussed optically thick films, where the modulation can result in extraordinary light transmission, the periodical modulation of ultrathin films can provide almost total suppression of the transmission. This effect is due to the resonance excitation of the short-range SPPs, which results also in up to 50% absorptivity and high reflectivity. Analogous anomalous effects could be observed in more complicated geometries and for variety parameters of the periodic films, for instance, those with dielectric filled slits and with $2D$ periodicity. We plan to discuss these cases in following publications.

ACKNOWLEDGMENT

The work was partially supported by STCU under Grant No. 3979.

*ak_04@rambler.ru

[1] T. W. Ebbesen *et al.*, Nature (London) **391**, 667 (1998).
[2] L. Martin-Moreno, F. J. Garcia-Vidal, H. J. Lezec, K. M. Pellerin, T. Thio, J. B. Pendry, and T. W. Ebbesen, Phys. Rev. Lett. **86**, 1114 (2001).
[3] H. Raether, *Surface Plasmons* (Springer-Verlag, Berlin, 1988).
[4] E. N. Economou, Phys. Rev. **182**, 539 (1969).
[5] Z. Chen, I. R. Hooper, and J. R. Sambles, Phys. Rev. B **77**, 161405(R) (2008).
[6] A. V. Kats and V. V. Maslov, Sov. Phys. JETP **35**, 264 (1972).
[7] A. V. Kats, P. D. Pavitskii, and I. S. Spevak, JETP **78**, 42 (1994).
[8] A. V. Kats, I. S. Spevak, and N. A. Balakhonova, Phys. Rev. B **76**, 075407 (2007).
[9] A. V. Kats, M. L. Nesterov, and A. Yu. Nikitin, Phys. Rev. B **76**, 045413 (2007); **72**, 193405 (2005).
[10] P. Lalanne and G. M. Morris, J. Opt. Soc. Am. A Opt. Image Sci. Vis. **13**, 779 (1996).
[11] L. Li, J. Opt. Soc. Am. A Opt. Image Sci. Vis. **13**, 1870 (1996).
[12] S. G. Rodrigo, F. J. Garcia-Vidal, and L. Martin-Moreno, Phys. Rev. B **77**, 075401 (2008).